

# Test particle modelling of ion collisional transport in tokamaks

Zhanna S. Kononenko,  
Yevgen O. Kazakov

**Abstract.** A numerical method is presented for evaluation of the radial diffusion coefficient, based on the full orbit modelling of particle orbits in the tokamak geometry. The code solves the full orbit equations of motion for a set of test particles in an arbitrary equilibrium magnetic field. The effect of Coulomb collisions of test ions with background plasma particles is simulated by means of an equivalent Monte Carlo collision operator which scatters the pitch angle as well as the gyrophase of the particle. The radial diffusion coefficient is estimated by calculating the temporal dependence of the mean-square displacement of an ensemble of monoenergetic test particles. As an illustration of the method the effect of magnetic islands on the impurity collisional transport is studied. It is shown that in presence of  $m = 2, n = 1$  resonant magnetic perturbation (RMP) the diffusion coefficient for the tungsten ions ( $W^{28+}, E = 1 \text{ keV}$ ) can increase by a factor of 5–10.

**Key words:** diffusion coefficient • impurity transport • magnetic islands • Monte Carlo collision operator • resonant magnetic perturbation (RMP) • test particle code

## Introduction

The test particle approach is widely used in fusion research to study the transport processes. With this method one may evaluate the transport (radial diffusion) coefficients [2, 10, 16], estimate the heat loads on different plasma-facing components [20], determine the poloidal and toroidal distributions of fast ion losses [8], clarify the effect of plasma rotation on plasma confinement [15], study the toroidal field (TF) ripple induced transport [4], analyze turbulent transport, when coupled with the electromagnetic turbulence code [19], etc.

In contrast to any analytical theory (such as the neoclassical theory or the drift kinetic equation [9]), test particle modelling is a direct numerical method to study the problems of plasma transport. Thus, no additional approximations concerning the Larmor radius of the particle, the aspect ratio of the machine, the ratio of the poloidal to toroidal components of the magnetic field need to be made. In principle, the method may be applied in any equilibrium magnetic field with a finite TF ripple, with arbitrary plasma density and temperature profiles, collisionality regime and other characteristics. The price that has to be paid for such an intrinsic simplicity is that the test particle modelling usually involves lengthy CPU-intensive calculations.

In this paper we describe a numerical code which evaluates the diffusion coefficient of a monoenergetic ensemble of test particles in the tokamak geometry.

Zh. S. Kononenko✉  
Faculty of Physics and Technology,  
V. N. Karazin Kharkiv National University,  
4 Svobody Sq., 61077 Kharkov, Ukraine,  
Tel.: +38 057 335 3610, Fax: +38 057 335 3610,  
E-mail: kononenko\_zh@mail.ru

Ye. O. Kazakov  
Department of Applied Physics,  
Nuclear Engineering Division,  
Chalmers University of Technology,  
Euratom-VR Association, Göteborg, Sweden

Received: 1 August 2011

Accepted: 21 November 2011

The full orbit integration is accompanied by the Monte Carlo collision operator which scatters both the pitch and gyro angles of the particle. As an exemplary application of this code we discuss how the magnetic islands produced by the resonant magnetic perturbation affect the collisional transport of impurities.

### Test particle code

Test particle codes used for the transport studies usually consist of two basic modules. The first module describes the deterministic motion of particles in the given magnetic configuration. Usually the particle trajectory integration module involves the use of the guiding center equations [2, 4, 16]. The effect of particle gyrorotation is often neglected, which results in a substantial reduction of the CPU time needed to trace a particle. Unfortunately, for some problems of interest this approximation cannot be applied. In such a case one has to solve the full orbit equations of motion. Such an approach should be used, for example, for studying the dynamics of alpha particles and fast ions with large Larmor radius [14]; recently this approach had been used to investigate the transport problems in spherical tokamaks [7, 15, 19]. For spherical torii the inverse aspect ratio,  $a/R_0$  ( $a$  – the minor plasma radius,  $R_0$  – the major radius of the torus) and the poloidal component of the magnetic field are no longer small parameters, thus the fundamental approximations of the neoclassical theory cannot be applied.

The full orbit equation of motion

$$(1) \quad m \frac{d\vec{v}}{dt} = \frac{q}{c} \vec{v} \times \vec{B}$$

is solved in the standard quasi-toroidal system of coordinates  $(r, \theta, \phi)$ , where  $r$  is the radial coordinate and  $\theta$  and  $\phi$  are the poloidal and toroidal angles, respectively. The equation of motion under the influence of the Lorentz force is written in the normalized form for six unknowns (three coordinates and three velocity components) in a form directly suitable for integration by an explicit Runge-Kutta scheme. Results reported in this paper were obtained with a standard RK4 method.

To speed up the calculations it is preferable to use an analytic expression for the magnetic field rather than the grid data obtained with the equilibrium magnetic field code based on the solution of the Grad-Shafranov equation (e.g., EFIT). In the present paper a simple tokamak magnetic field model is used [6], which gives circular magnetic surfaces:

$$(2) \quad \vec{B} = \frac{B_0 R_0}{R} \left[ \vec{e}_\phi + \frac{r/R_0}{q(r) \sqrt{1 - (r/R_0)^2}} \vec{e}_\theta \right]$$

where  $q(r)$  is the safety factor and  $R = R_0 + r \cos\theta$ . The profile of  $q(r)$  used in our calculations is shown in Fig. 1.

The second module of the code describes the stochastic scattering of test particles due to the Coulomb collisions with background plasma particles. Usually Monte Carlo equivalent collision operators are used to this end, which randomly change the velocity of the

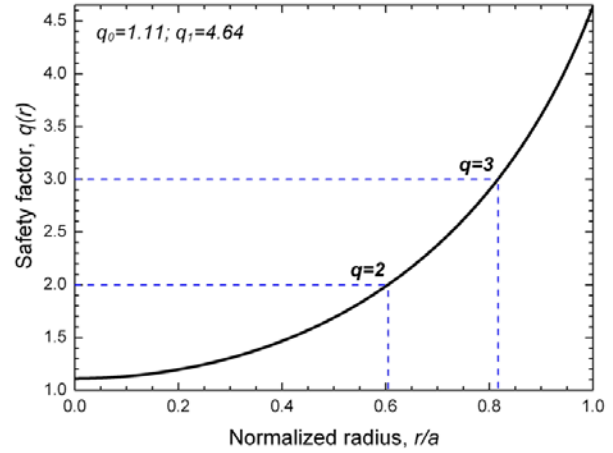


Fig. 1. The safety factor profile,  $q(r)$ .

particle after each time step of the integration procedure. In calculations based on guiding center equations it is sufficient to use a collision operator that changes the pitch angle of the particle only [2]. However, for the full orbit modelling an implementation of the scattering of both of the particle pitch angle and the gyrophase is needed. A Monte Carlo collision operator suitable for exact trajectory integrators was derived by Boozer in [1]:

$$(3) \quad \vec{v}_n = (1 - v_d \Delta t) \vec{v}_0 \pm \sqrt{(1 - 0.5 v_d \Delta t) v_d \Delta t} (\vec{\pi}_0 \pm \vec{\tau}_0) v_0$$

where  $\vec{b}$  is the unit vector along the magnetic field;  $\vec{v}_0$  and  $\vec{v}_n$  are the velocities of the particle before and after the scattering, respectively;  $\vec{\pi}_0 = [(\vec{b} \times \vec{v}_0) / (|\vec{b} \times \vec{v}_0|)]$  and  $\vec{\tau}_0 = (\vec{\pi}_0 \times \vec{v}_0) / v_0$  are two unit vectors perpendicular to  $\vec{v}_0$ . Here,  $v_d$  is the collision frequency and  $\Delta t$  is the time step used in the code chosen to satisfy  $v_d \Delta t \ll 1$ . In contrast to the guiding center Monte Carlo collision operator the full orbit operator involves two random numbers for each particle at each time step. The sign plus or minus in Eq. (3) should be chosen randomly, but with equal probabilities. A Monte Carlo operator of the form (3) ensures that after sufficiently long time particle spends equal time at all values of the pitch and gyro angles. An important feature of the operator (3) is that it changes only the direction of the velocity, but not its magnitude.

For the field particles with a Maxwellian distribution the deflection frequency appearing in the collision operator is defined as follows [2, 9]:

$$(4) \quad \nu_d^{\alpha/\beta} = \nu_0^{\alpha/\beta} \left[ \Phi(x^{\alpha/\beta}) - G(x^{\alpha/\beta}) \right]$$

Here the indices  $\alpha$  and  $\beta$  test and background plasma particles, respectively. The reference deflection frequency in Eq. (4) is given by:

$$(5) \quad \nu_0^{\alpha/\beta} = \frac{4\pi q_\alpha^2 q_\beta^2 n_\beta \ln \Lambda_{\alpha\beta}}{m_\alpha^2 v_\alpha^3} \approx \frac{28.5 Z_\alpha^2 Z_\beta^2 n_\beta [10^{13} \text{ cm}^{-3}] \ln \Lambda_{\alpha\beta}}{A_\alpha^{1/2} (T_\alpha [\text{keV}])^{3/2}}$$

where:  $\Phi(x) = \frac{2}{\sqrt{\pi}} \int_0^x e^{-t^2} dt$  is the error function;

$G(x) = \frac{\Phi(x) - x\Phi'(x)}{2x^2}$  is the Chandrasekhar function,

and the argument of the functions in Eq. (4) is the ratio

of the test particle velocity to the thermal velocity of the background species. If one considers the scattering of heavy impurities whose atomic mass is large compared with that of bulk ions, then in the limit  $x^{\alpha/\beta} \ll 1$  the expression for the deflection frequency simplifies to:

$$(6) \quad v_d^{\alpha/\beta} = \frac{4x^{\alpha/\beta}}{3\sqrt{\pi}} v_0^{\alpha/\beta}$$

For the tungsten ions ( $W^{28+}$ ) with the energy  $E = 1$  keV scattered in deuterium plasma ( $T_i = 3$  keV,  $n_i = 2.5 \times 10^{13} \text{ cm}^{-3}$ ), the collision frequency is  $v_d \approx 3.4 \times 10^3 \text{ s}^{-1}$ . Highly charged impurities are more collisional than bulk plasma particles.

In order to evaluate the diffusion coefficient the full orbit equations of motion for an ensemble of  $N = 1000$  monoenergetic particles are solved, applying at each time step velocity change according to Eq. (3). All particles evolve independently from each other. They start their motion from the flux surface where  $q = 2$  ( $r_0/a \approx 0.604$ ). The initial poloidal and toroidal angles of each particle are distributed randomly, as well as the velocity components. The statistical properties of the ensemble are characterized by means of the mean-square displacement:

$$(7) \quad C_2(t) = \langle (r_i(t) - \langle r(t) \rangle)^2 \rangle$$

where brackets denote an average over the particles in the ensemble. The diffusion coefficient is defined as the time derivative of the mean-square displacement:

$$(8) \quad D(t) = \frac{1}{2} \frac{dC_2(t)}{dt}$$

The temporal dependence of  $C_2$  defines the type of diffusion. For normal diffusion processes the mean-square displacement increases linearly in time. Figure 2 shows a typical temporal dependence of the mean-square displacement for the ensemble of  $W^{28+}$  ions with the energy  $E = 1$  keV. The integration time in our simulations is chosen to be 10 collision times, which is equal to 3 ms for the considered case. As follows from Fig. 2, for time intervals smaller than the mean time between the collisions there is a ballistic phase when

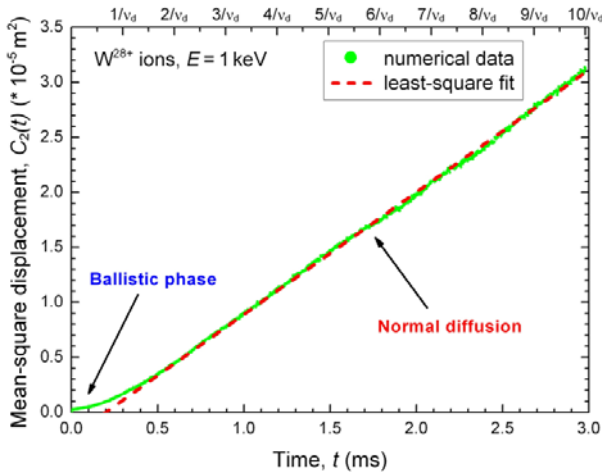


**Fig. 2.** A typical temporal dependence of the mean-square displacement,  $C_2(t)$ , for the ensemble of  $N = 1000$   $W^{28+}$  ions with the energy  $E = 1$  keV.

$C_2(t)$  varies quadratically in time. Then, the collisional effects start to dominate and the normal diffusion is observed. The diffusion coefficient is calculated as a slope of the curve for the mean-square displacement. Fitting the curve by the least-squares method we find that the relative accuracy of the  $D$  coefficient estimated in this way is approximately 10%. The accuracy of  $D$  may be improved by increasing the number of particles in the ensemble; the noise in the curve  $C_2(t)$  scales inversely with the square root of the number of particles [19].

The obtained results are in a fair agreement with the results of the neoclassical theory [13]. The diffusion coefficient has been calculated for several impurity species:

$$\begin{aligned} W^{28+}, \quad E = 1 \text{ keV}, \quad & D_{\text{num}} = 5.5 \times 10^{-3} \text{ m}^2/\text{s} \\ & (D_{\text{neo}} = 4.1 \times 10^{-3} \text{ m}^2/\text{s}); \\ C^{6+}, \quad E = 1 \text{ keV}, \quad & D_{\text{num}} = 1.3 \times 10^{-2} \text{ m}^2/\text{s} \\ & (D_{\text{neo}} = 1.2 \times 10^{-3} \text{ m}^2/\text{s}); \\ W^{46+}, \quad E = 5 \text{ keV}, \quad & D_{\text{num}} = 9.9 \times 10^{-3} \text{ m}^2/\text{s} \\ & (D_{\text{neo}} = 8.8 \times 10^{-3} \text{ m}^2/\text{s}). \end{aligned}$$

For the considered parameters the impurities are in the Pfirsch-Schlüter ( $W^{28+}$ ) or the plateau regime ( $C^{6+}$ ,  $W^{46+}$ ). The values obtained from numerical calculations are somewhat higher than the neoclassical values, especially for the highly ionized tungsten species.

### Effect of the magnetic islands on the collisional transport of impurities

The full orbit test particle code had been used to study the effect of resonant magnetic perturbations (RMP's) on the collisional transport of impurities. RMP's are actively studied in view of the perspective of their use for ELM active control and suppression [5, 12]. The additional coils producing a perturbation to the equilibrium magnetic field are installed on many present-day tokamaks: DIII-D, JET, MAST, NSTX, TEXTOR, as well as stellarators. Such a system is also considered for the installation at the ITER tokamak [18].

In theoretical studies the magnetic field perturbation is usually introduced as follows [3]:

$$(9) \quad \delta \vec{B} = \vec{\nabla} \times (\alpha \vec{B}_0)$$

where the scalar function  $\alpha = \alpha(r, \theta, \phi)$  (which has the physical dimension of length) defines the structure of the perturbed magnetic field. For the present study we consider a single harmonic perturbation of the form [17]:

$$(10) \quad \alpha(r, \theta, \phi) = \alpha_0 e^{-(r-r_{\text{res}})/\Delta_{\text{res}})^2} \sin(m\theta - n\phi)$$

This perturbation produces a chain of  $m$  magnetic islands with a center at the rational magnetic surface ( $r = r_{\text{res}}$ ) where  $q = m/n$ . The magnetic perturbation of the form (10) produces only a single chain of magnetic islands, avoiding the formation of satellite islands. The effect of the island overlapping on the diffusion behavior was studied in [17]. In the present paper we focus our attention on the effect of the  $m = 2, n = 1$  perturbation on the impurity diffusion which produces a single chain of two magnetic islands in the poloidal cross-section (Fig. 3).

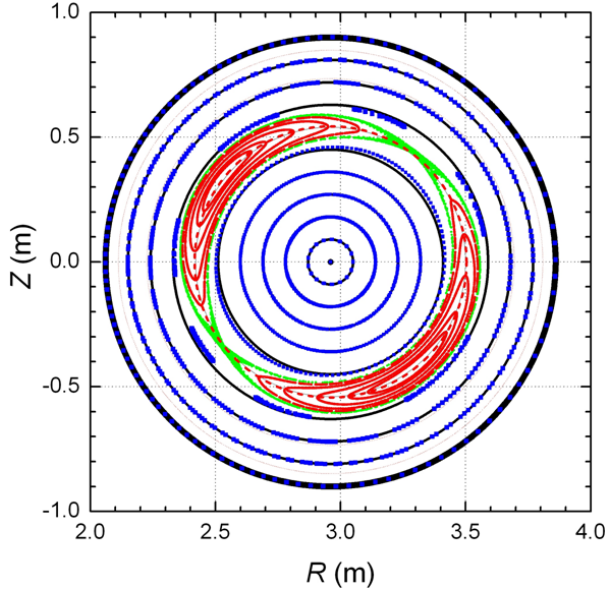


**Fig. 3.** A Poincaré plot of the perturbed magnetic field ( $\phi = 0$ ). A chain of two magnetic islands is created due to the splitting of the rational magnetic surface at the point where  $q = 2$ .

The radial width of the magnetic islands is controlled by the RMP amplitude and is approximately given by [21]:

$$(11) \quad \delta r \approx 4q \sqrt{\frac{\alpha_{00} R_0}{r(dq/dr)}}$$

where the shear  $dq/dr$  is evaluated at  $r = r_{\text{res}}$ . Figure 4 shows that the perturbation with the normalized amplitude  $\alpha_{00}/a = 10^{-4}$  produces magnetic islands with a width  $\sim 10\%$  of the plasma radius.

Figure 5 presents the time dependence of the mean-square displacement for tungsten ions ( $W^{28+}$ ), for different perturbation amplitudes. The lowest curve corresponds to the case of the plasma without magnetic islands. As expected, an increase in RMP amplitude results in greater radial displacements of particle orbits and hence bigger diffusion coefficient. The observed diffusion is normal in all cases since collisions are rather frequent. For the regimes of reduced collisionality the radial particle transport under the presence of magnetic islands can exhibit sub-diffusive or non-diffusive behavior [11, 17].

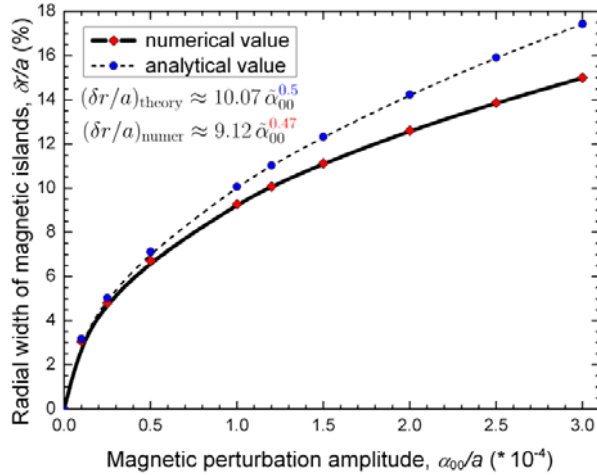


**Fig. 4.** The radial width of the magnetic islands as a function of the RMP amplitude.

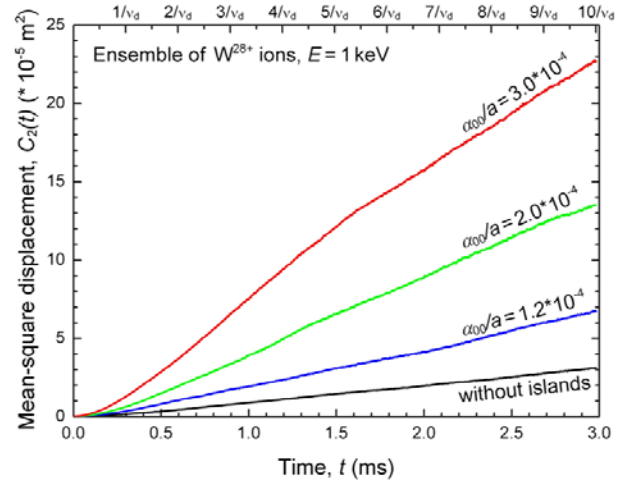


**Fig. 5.** The temporal dependence of the mean-square displacement,  $C_2(t)$ , of  $W^{28+}$  ions for different magnetic perturbation amplitudes.

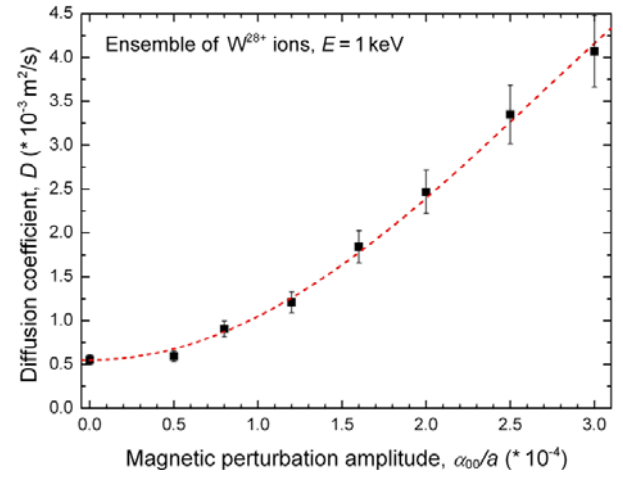


**Fig. 6.** The diffusion coefficient for  $W^{28+}$  ions as a function of the magnetic perturbation amplitude.

Figure 6 summarizes the obtained results. It shows how the diffusion coefficient for the  $W^{28+}$  impurities depends on the RMP amplitude. Under the assumption that the characteristic radial displacement of the particle is simply proportional to the island width the curve in Fig. 6 should be linear in  $\alpha_{00}$ . However, the observed curve shows a more complex quadratic dependence of the diffusion coefficient on the RMP amplitude. For the case when the island width is 15% of the plasma radius the diffusion coefficient for  $W^{28+}$  ions increases by a factor of 8 with respect to the case without perturbation.

## Summary and conclusions

A numerical method to evaluate the radial diffusion coefficient of test particles in a tokamak geometry is described in detail. The Coulomb collisions of test particles with the background plasma are modelled by means of an equivalent Monte Carlo collision operator scattering both the pitch and gyro angles of the particle. Diffusion coefficients obtained from numerical simulation are in a fair agreement with the results of the neoclassical theory. It is shown that the impurity

diffusion coefficient may be significantly enhanced by magnetic islands produced by the RMP's.

**Acknowledgment.** The work of Zh. S. Kononenko was partially supported by the Erasmus Mundus Visiting Scientist Scholarship. This work was also partly funded by the European Communities under Association Contract between EURATOM and Vetenskapsrådet. The views and opinions expressed herein do not necessarily reflect those of the European Commission.

## References

1. Boozer AH (2002) Monte Carlo collision operators for use with exact trajectory integrators. *Phys Plasmas* 9:4389–4391
2. Boozer AH, Kuo-Petravic G (1981) Monte Carlo evaluation of transport coefficients. *Phys Fluids* 24:851–859
3. Boozer AH, White RB (1982) Particle diffusion in tokamaks with partially destroyed magnetic surfaces. *Phys Rev Lett* 49:786–789
4. Bustos A, Castejón F, Fernández LA *et al.* (2010) Impact of 3D features on ion collisional transport in ITER. *Nucl Fusion* 50:125007
5. Evans TE, Moyer RA, Burrell KH *et al.* (2006) Edge stability and transport control with resonant magnetic perturbations in collisionless tokamak plasmas. *Nature Physics* 2:419–423
6. Freidberg J (2007) *Plasma physics and fusion energy*. Cambridge University Press, Cambridge
7. Gates DA, Mynick HE, White RB (2004) Collisional transport in a low aspect ratio tokamak. *Phys Plasmas* 11:L45–L48
8. Gobbin M, Marrelli L, Fahrbach HU *et al.* (2009) Numerical simulations of fast ion loss measurements induced by magnetic islands in the ASDEX Upgrade tokamak. *Nucl Fusion* 49:095021
9. Helander P, Sigmar DJ (2002) *Collisional transport in magnetized plasmas*. Cambridge University Press, Cambridge
10. Kononenko ZhS, Shishkin AA (2008) Impurity ion dynamics near magnetic islands in the drift optimized stellarator configuration of Wendelstein 7-X. *Ukr J Phys* 53:437–441
11. Kononenko ZhS, Shishkin AA (2008) The influence of magnetic islands on the impurity ion motion in the drift optimized stellarator. *Probl Atom Sci Tech* 4:95–98
12. Liang Y, Koslowski HR, Thomas PR *et al.* (2007) Active control of type-I edge localized modes on JET. *Plasma Phys Control Fusion* 49:B581–B590
13. Lotz W, Nührenberg J (1988) Monte-Carlo computations of neoclassical transport. *Phys Fluids* 31:2984–2991
14. McClements KG (2005) Full orbit computations of ripple-induced fusion  $\alpha$ -particle losses from burning tokamak plasmas. *Phys Plasmas* 12:072510
15. McKay RJ, McClements KG, Thyagaraja A, Fletcher L (2008) Test-particle simulations of collisional impurity transport in rotating spherical tokamak plasmas. *Plasma Phys Control Fusion* 50:065017
16. Maluckov A, Nakajima N, Okamoto M, Murakami S, Kanno R (2001) Statistical properties of the neoclassical radial diffusion in a tokamak equilibrium. *Plasma Phys Control Fusion* 43:1211–1226
17. Maluckov A, Nakajima N, Okamoto M, Murakami S, Kanno R (2003) Statistical properties of the radial transport in the magnetic field with radially bounded stochastic region. *Physica A* 322:13–37
18. Nardon E, Bécoulet M, Huysmans G *et al.* (2007) Edge localized modes control by resonant magnetic perturbations. *J Nucl Mater* 363/365:1071–1075
19. Romanelli M, McClements KG, Cross J, Knight PJ, Thyagaraja A, Callaghan J (2011) Full orbit simulation of collisional transport of impurity ions in the MAST spherical tokamak. *Plasma Phys Control Fusion* 53:054017
20. Strumberger E (2000) Deposition patterns of fast ions on plasma facing components in W7-X. *Nucl Fusion* 40:1697–1713
21. Wesson J (2004) *Tokamaks*. Clarendon Press, Oxford